


# Knockdown of Immature Colon Carcinoma Transcript I Inhibits Proliferation and Promotes Apoptosis of Non–Small Cell Lung Cancer Cells

Technology in Cancer Research & Treatment  
2017, Vol. 16(5) 559–569  
© The Author(s) 2016  
Reprints and permission:  
sagepub.com/journalsPermissions.nav  
DOI: 10.1177/1533034616657977  
journals.sagepub.com/home/tct  


Yiling Wang, MM<sup>1</sup>, Jiantao He, MM<sup>1</sup>, Shenghui Zhang, MM<sup>1</sup>,  
Qingbo Yang, MM<sup>1</sup>, Bo Wang, MM<sup>1</sup>, Zhiyu Liu, MM<sup>1</sup>,  
and Xintian Wu, MM<sup>1</sup>

## Abstract

Non–small cell lung cancer, as the most frequent type lung cancer, has lower survival rate of 5 years, despite improvements in surgery and chemotherapy. Previous studies showed immature colon carcinoma transcript I is closely related to tumorigenesis of human cancer cells. In the present study, we found immature colon carcinoma transcript I was overexpressed in lung cancer tissues using Oncomine database mining, and the biological effect of immature colon carcinoma transcript I was investigated in non–small cell lung cancer cell lines 95D and A549. Lentivirus-mediated RNA interference was used to knock down immature colon carcinoma transcript I expression in 95D and A549 cells *in vitro*, and the knockdown efficiency was determined using quantitative real-time polymerase chain reaction and Western blot assay. Knockdown of immature colon carcinoma transcript I significantly suppressed non–small cell lung cancer cell proliferation and colony formation ability confirmed by 3-(4,5-dimethylthiazol-2-yl)-2,5-diphenyltetrazolium bromide and colony formation assay. Flow cytometry was applied to measure cell cycle arrest, and the result showed the cell cycle arrested in G<sub>2</sub>/M phase in 95D cells and arrested in G<sub>0</sub>/G<sub>1</sub> phase in A549 cells. Furthermore, we measured the levels of cell cycle–associated proteins by Western blot analysis and found immature colon carcinoma transcript I–mediated cell proliferation inhibition appeared due to downregulation of cell cycle activator cyclin D1 and upregulation of cell cycle inhibitor p21. In addition, immature colon carcinoma transcript I silencing significantly induced non–small cell lung cancer cell apoptosis by annexin V/7-amino-actinomycin D double-staining assay. All our data suggest that immature colon carcinoma transcript I may play an important role for non–small cell lung cancer cell proliferation and could be a potential molecular target for diagnosing and treating human non–small cell lung cancer.

## Keywords

*ICT1*, NSCLC, cell cycle, cell proliferation, RNAi

## Abbreviations

cDNA, complementary DNA; DMEM, Dulbecco modified eagle medium; FBS, fetal bovine serum; GBM, glioblastoma multiforme; GFP, green fluorescence protein; *ICT1*, immature colon carcinoma transcript I; LC, lung cancer; mRNA, messenger RNA; NC, negative control; NSCLC, non–small cell lung cancer; PCR, polymerase chain reaction; PI, propidium iodide; qRT-PCR, quantitative real-time polymerase chain reaction; RNAi, RNA interference; SD, standard deviation; shRNA, short hairpin RNA

Received: October 21, 2015; Revised: April 14, 2016; Accepted: June 06, 2016.

## Introduction

Lung cancer (LC) is one of the most frequently diagnosed cancer and a leading cause of tumor-related death worldwide.<sup>1,2</sup> Clinically, LC is divided into 2 major histologic categories, including small-cell lung cancer and non–small cell lung cancer (NSCLC).<sup>3</sup> Non–small cell lung cancer, as locally advanced disease, could account for 80% of LC cases with 15%

<sup>1</sup> Department of Thoracic Surgery, Shanghai Tenth People's Hospital, Shanghai, China

### Corresponding Author:

Yiling Wang, MM, Department of Thoracic Surgery, Shanghai Tenth People's Hospital, No. 301 Yanchangzhong Rd, Shanghai 200072, China.  
Email: elliotwang2004@126.com

survival rate for 5 years, despite improvements in surgery and chemotherapy.<sup>4</sup> The conventional chemotherapy has made NSCLC generate drug resistance. Recently, gene therapy methods have been widely evaluated in clinical trials and considered as potential value for the treatment of cancer.<sup>5</sup> Therefore, it may bring better outcome for LC to identify novel genes along with the conventional therapies.

Immature colon carcinoma transcript 1 (*ICT1*) is an essential mitochondrial protein and an integral component of the human mitoribosome.<sup>6</sup> Richter *et al* has reported *ICT1* might be essential for hydrolysis of prematurely terminated peptidyl-tRNA moieties in mitoribosome.<sup>6</sup> The *ICT1* knockdown decreased cytochrome c oxidase activity by 35% and suppressed mitochondrial membrane potential and mass,<sup>7</sup> which suggested *ICT1* is indispensable to mitochondrial activities. In addition, *ICT1* is essential for cell vitality. Increasing evidence show *ICT1* knockdown significantly inhibits cell proliferation in prostate cancer<sup>8</sup> and glioblastoma multiforme (GBM).<sup>9</sup> *ICT1* has been identified as a hug gene for LC and guessed to play an important role in the progression of LC.<sup>10</sup> However, its role in LC has not been further investigated.

Recently, RNA interference (RNAi) has been widely thought as a powerful tool, which was used to study the target genes involved in cancer progression. To explore the biological effect of *ICT1* in LC, the expression *ICT1* was successfully silenced in the NSCLC cell lines 95D and A549 using RNAi technology. What's more, the biological effect of *ICT1* knockdown was evaluated via cell proliferation, colony formation, cell cycle analysis, and cell apoptosis, as well as underlying molecular mechanism.

## Materials and Methods

### Data Mining and Oncomine Analysis

Publicly online Oncomine cancer microarray database (www.oncomine.com) was used to explore the expression levels of *ICT1* in LC tissues.<sup>11</sup> The *ICT1* differential expressions between LC and normal lung specimens were digged from 8 different databases including Bhattacharjee Lung,<sup>12</sup> Landi Lung,<sup>13</sup> Beer Lung,<sup>14</sup> Stearman Lung,<sup>15</sup> Su Lung,<sup>16</sup> Hou Lung,<sup>17</sup> Selamat Lung,<sup>18</sup> and Okayama Lung.<sup>19</sup> The *ICT1* expression levels between LC and normal tissues were compared as previously described.<sup>20</sup>

### Cell Lines and Cell Culture

Human LC cell lines 95D, A549, H1299, H460, SPC-A-1 and human embryonic kidney cells 293T (HEK293T) were provided by the Cell Bank of Chinese Academy of Science (Shanghai, China). The 95D, H1299, H460, and SPC-A-1 cells were maintained in RPMI-1640 (Hyclone, Logan, UT, USA) supplemented with 10% fetal bovine serum (FBS, Biowest, Loire Valley, France). A549 and HEK293T cells were cultured in Dulbecco modified eagle medium (DMEM; Hyclone, Logan, UT, USA) plus 10% FBS. These cell lines were incubated in a humidified atmosphere containing 5% CO<sub>2</sub>.

### Lentivirus Packaging and Transduction

Two short hairpin RNA (shRNA) sequences targeting human *ICT1* gene (NM\_001146108.1) were designed as follows: 5'-GCTGTTAATGCTTGTCTATAACTCGAGTTATAGCAAGCATTAAACAGCTTTTTT-3' (S1) and 5'-GCAGAATGTGAACAAAGTGAAGTCTCGAGTTCAGTTTGTTCATTCTGCTTTTTT-3' (S2). A scrambled shRNA sequence (5'-GATCCTTCTCCGAACGTGTACGTCTCGAGACGACGCACTGGCGGAGAATTTTTG-3') was used as a negative control (NC). Then, the shRNAs were inserted into the pFH-L lentiviral vector containing a green fluorescence protein (GFP) reporter (Shanghai Hollybio, China) between *NheI* and *PacI* restriction sites and then confirmed by DNA sequencing. The constructed lentiviral vector plasmids were named as pFH-L-shICT1(S1), pFH-L-shICT1(S2), or pFH-L-NC. Before transfection, HEK293T cells were inoculated in 10-cm cell culture dishes and cultured for 24 hours to reach 70% to 80% cell density. Two hours before transfection, the medium was replaced by the basic medium (without serum and antibiotics). Subsequently, 10 µg constructed plasmid (pFH-L-shICT1 or pFH-L-NC), helper plasmids 7.5 µg pCMVΔR8.92, and 5 µg pVSVG-I (Shanghai Hollybio) were mixed with the corresponding volume of serum-free DMEM. After incubated for 5 minutes, 50 µL of Lipofectamine 2000 (Invitrogen, Carlsbad, CA, USA) was added into the aforementioned mixture according to the manufacturer's instructions. HEK293T cells were cocultured with the transfection mixture for 6 hours and replaced the medium by the DMEM medium with 10% FBS. Two days after transfection, the supernatant was collected, centrifuged for 10 minutes (4000g, 4°C), and filtered through a 0.45-µm cellulose acetate filter to obtain the lentiviral particles. The recombinant lentivirus was stored at -80°C.

The 95D cells (80 000 cells/well) and A549 cells (50 000 cells/well) were dispensed into 6-well plates and transduced with shRNA-expressing lentivirus with a multiplicity of infection of 6 for 95D cells and 20 for A549 cells, respectively. Infection efficiency was measured by counting the numbers of GFP-positive cells under fluorescence microscope at 96 hours after infection.

### Knockdown Efficiency Determination by Quantitative Real-Time Polymerase Chain Reaction

The 95D and A549 cells were divided into 3 groups including NC cells, shICT1(S1), and shICT1(S2). All cells were harvested after lentivirus transduction for 5 days and then extracted total cellular RNA using TRIzol reagent (Life technologies, Carlsbad, CA, USA), according the manufacturer's instructions. Complementary DNA (cDNA) was synthesized from obtained RNA (2 µg) using M-MLV reverse transcriptase kit (Promega, Madison, WI, USA), of which the Oligo (dT)<sub>18</sub> primer (5'-d(TTTTTTTTTTTTTTTTTT)-3') was used. In addition, primers (forward: 5'-CAGCCTGGACAAGCTCTACC-3' and reverse: 5'-GGAACCTGACTTCTGCCTTG-3') were designed to determine the expression of *ICT1*. Actin (forward: 5'-GTGGA CATCCGCAAAGAC-3' and reverse: 5'-AAAGGGTGTAAACG CAACTA-3') was used as endogenous control.

The *ICT1* messenger RNA (mRNA) level was measured on Bio-Rad Connect real-time polymerase chain reaction (PCR) platform with 20  $\mu$ L PCR mixture (10  $\mu$ L 2  $\times$  SYBR Premix Ex Taq, 0.5  $\mu$ L primers [2.5  $\mu$ mol/L], 5  $\mu$ L cDNA [30 ng/ $\mu$ L], and 4.5  $\mu$ L ddH<sub>2</sub>O). The detailed PCR procedure was initially denatured at 95°C for 1 minute, 40 cycles of denaturation at 95°C for 5 seconds, and extension at 60°C for 20 seconds. The absorbance values were read at the extension stage and used to analyze the relative quantitation of *ICT1* between C(T) of actin and C(T) of *ICT1* using  $2^{-\Delta\Delta C_t}$  formula.<sup>21</sup>

### 3-(4,5-dimethylthiazol-2-yl)-2,5-diphenyltetrazolium bromide (MTT) for Cell Viability Analysis

To evaluate the effect of *ICT1* on 95D and A549 cell viability, MTT assay was performed in 95D and A549 cells from different groups (NC, sh*ICT1*[S1], and sh*ICT1*[S2]), according to the previous report.<sup>22</sup> Briefly, cells were plated in 96-well plates at a density of 3500 cells/well in 95D and 2000 cells/well in A549. Then, 20  $\mu$ L MTT solution was added into each well at different time points (1, 2, 3, 4, and 5 days) after incubation and then incubated for 4 hours at 37°C. Afterward, each well was added 100  $\mu$ L acidic isopropanol (5% isopropanol, 10% sodium dodecyl sulfate [SDS], and 0.01 mol/L HCl) and then incubated for overnight at 37°C. The absorbance of each plate was measured with an enzyme-linked immunosorbent assay reader (Bio-Rad, Hercules, CA, USA) at a wavelength of 595 nm.

### Colony Formation Assay

To determine cell growth, the colony formation analysis was performed on 95D and A549 cells from different groups (NC, sh*ICT1*[S1], and sh*ICT1*[S2]). Briefly, lentiviral-infected cells were seeded in 6-well plate at a density of 400 cells/well in 95D and A549. Eight days after culture, cells were fixed with 4% paraformaldehyde and then stained with crystal violet as described in previous report.<sup>23</sup> The number of colonies (more than 50 cells) was counted under the fluorescence microscope.

### Cell Cycle Analysis

To evaluate the effect of *ICT1* on cell cycle progression, flow cytometry assay was performed in 95D and A549 cells from 2 groups (NC and sh*ICT1*[S1]) after lentivirus transduction for 5 days. Briefly, 95D and A549 cells were seeded into 6-cm dishes at a density of 80 000 cells/dish and then cultured for 5 days to reach 80% confluence. Afterward, cells were collected, fixed in precold 70% ethanol, and then digested with RNase. The cells were stained with propidium iodide (PI) and analyzed cell cycle distribution using a flow cytometer (FACS-Calibur; BD Biosciences, San Jose, CA, USA).

### Protein Extraction and Western Blot

After lentivirus transduction for 5 days, 95D and A549 cells were harvested and lysed in 2 $\times$  SDS sample buffer (10 mmol/L

EDTA, 100 mmol/L Tris-HCl [pH 6.8], 4% SDS, and 10% glycine). The concentration of total protein was determined by the bicinchoninic acid assay. Quantitative 30  $\mu$ g proteins were separated by polyacrylamide–SDS electrophoresis for 3 hours at 60 V and then transferred to polyvinylidene fluoride (PVDF) membranes. The membranes were blocked with 5% nonfat milk in Tris-buffered saline with 0.05% Tween for 1 hour at room temperature and then blotted with primary antibodies, including anti-*ICT1* (1:1000, #AP20382b; Abgent, San Diego, CA, USA), anti-p21 (1:1000, #2947; Cell signaling, Danvers, MA, USA), anti-cyclin D1 (1:1000, 60186-1-1g; Proteintech, Chicago, IL, USA), and anti-glyceraldehyde 3-phosphate dehydrogenase (1:500 000, 10494-1-AP; Proteintech, Chicago, IL, USA) overnight at 4°C, followed by incubation with horseradish peroxidase-conjugated goat antirabbit (1:5000, Santa Cruz, SC-2054, Dallas, TX, USA) for 1 hour at room temperature. The enhanced chemiluminescence kit (Amersham, GE Healthcare Bio-Sciences, Pittsburgh, PA, USA) was used to detect the blots, according to the manufacturer's instruction. Glyceraldehyde 3-phosphate dehydrogenase was used as the internal standard.

### Annexin V/7-amino-actinomycin D (7-AAD) Double-Staining Analysis

To investigate the cell apoptosis, annexin V-APC/7-AAD double staining was performed. After lentivirus infection 5 days, the 95D and A549 cells from different groups (NC, sh*ICT1*[S1], and sh*ICT1*[S2]) were reseeded in 6-cm dishes at a density of 80 000 cells/dish. After 48 hours, the cells were collected and processed using annexin V-APC/7-AAD apoptosis kit (KeyGen Biotech, Nanjing, China), according to the manufacturer's instructions. Subsequently, cells were analyzed using a Cell Quest FACS system (BD Biosciences, San Jose, CA, USA).

### Statistical Analysis

All data were analyzed by SPSS software version 10.0 (SPSS, Inc, Chicago, IL, USA) and presented as mean (standard deviation) (SD) of 3 independent experiments. Paired Student *t* test was used to compare differences between groups. Statistically significant differences were defined as  $P < .05$ .

## Results

### Immature Colon Carcinoma Transcript 1 mRNA Expression Was Overexpressed in LC

To investigate the expression levels of *ICT1* in LC, we analyzed the Oncomine cancer microarray database. As shown in Figure 1A, Bhattacharjee Lung data set showed that *ICT1* expression is significantly increased in lung adenocarcinoma ( $n = 139$ ,  $P = 9.56E^{-4}$ ), small-cell lung carcinoma ( $n = 6$ ,  $P = 2.90E^{-2}$ ), and squamous cell lung carcinoma ( $n = 21$ ,  $P = 3.30E^{-2}$ ) compared with the normal tissues and was slightly upregulated in lung carcinoid tumor ( $n = 20$ ). We also found that the expression level of *ICT1* was also significantly

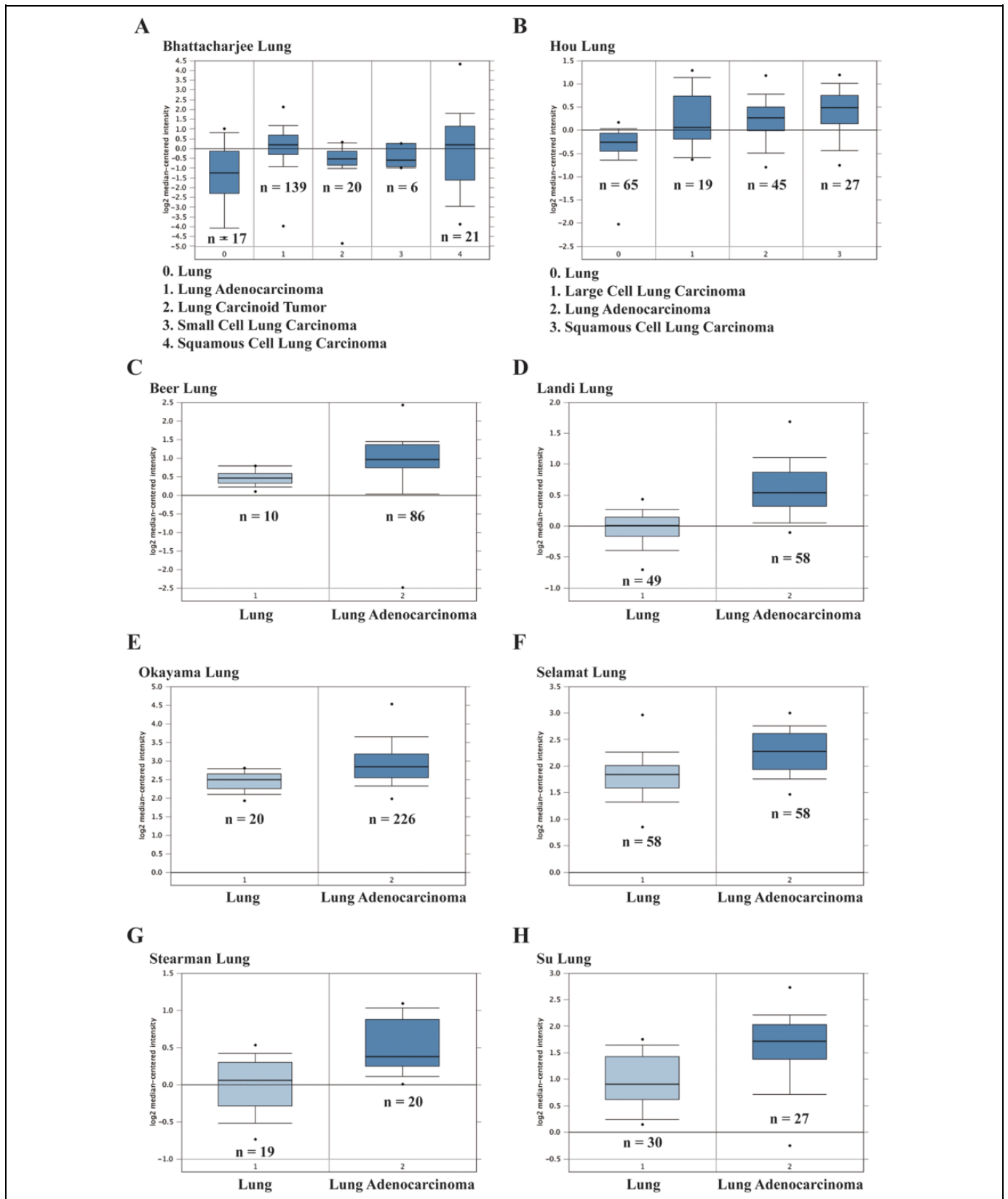


**Figure 1.** Immature colon carcinoma transcript 1 (ICT1) messenger RNA (mRNA) expression level in lung cancer (LC) was analyzed by Oncomine database. The expression level of ICT1 gene acquired from (A) Bhattacharjee lung data set, (B) Hou Lung data set, (C) Beer Lung data set, (D) Landi Lung data set, (E) Okayama Lung data set, (F) Selamat Lung data set, (G) Stearman Lung data set, and (H) Su Lung data set was shown as histograms, respectively. The total number of specimens was shown under each histogram.

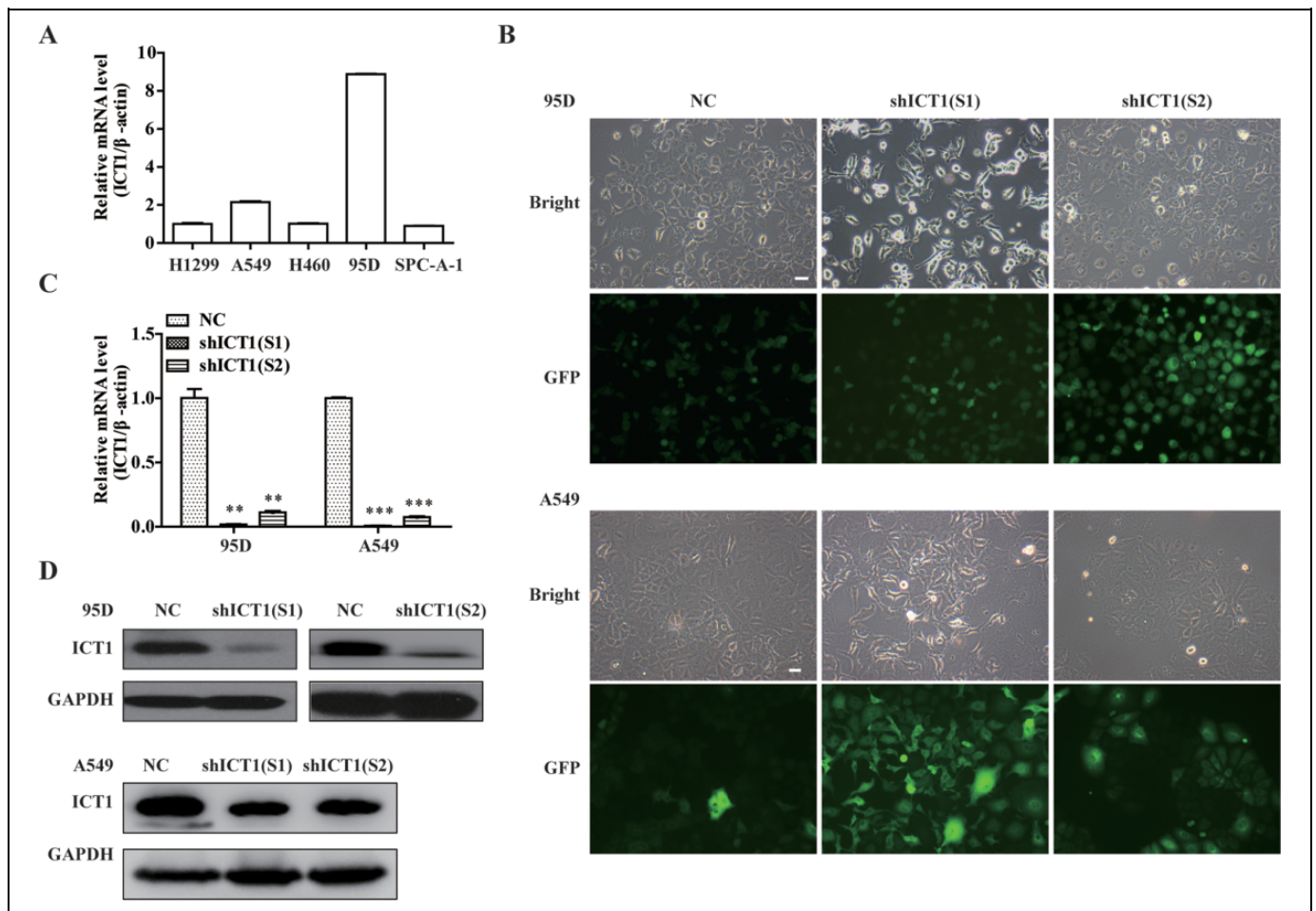


**Figure 2.** Knockdown of immature colon carcinoma transcript 1 (*ICT1*) expression in non-small cell lung cancer (NSCLC) cells. **A**, The expression level of *ICT1* was examined in 5 of lung cells line by quantitative real-time polymerase chain reaction (qRT-PCR). **B**, Representative images recorded under a fluorescence microscope of 95D and A549 cells infected with 2 *shICT1* lentivirus for 96 hours. **C**, The 95D and A549 cells were transfected with negative control (NC) or *shICT1* group for 5 days. Knockdown efficiency of *ICT1* was confirmed by quantitative real-time PCR. **D**, Total cellular proteins were extracted 5 days after infection with NC or *shICT1* group in 95D and A549 cells, and knockdown efficiency was assayed by Western blotting. \*\* $P < .01$ ; \*\*\* $P < .001$ ; scale bar, 10  $\mu\text{m}$ .

higher in 3 LC types including large-cell lung carcinoma ( $n = 19$ ,  $P = 7.41E^{-4}$ ), lung adenocarcinoma ( $n = 45$ ,  $P = 2.04E^{-9}$ ), and squamous cell lung carcinoma ( $n = 27$ ,  $P = 5.18E^{-9}$ ) than the normal tissues in Hou Lung data set (Figure 1B). Furthermore, *ICT1* expression in lung adenocarcinoma tissues is remarkably upregulated as shown in 6 different microarray data sets including Beer Lung ( $n = 86$ ,  $P = 8.81E^{-5}$ ), Landi Lung ( $n = 58$ ,  $P = 2.92E^{-16}$ ), Okayama Lung ( $n = 226$ ,  $P = 1.90E^{-8}$ ), Selamat Lung ( $n = 58$ ,  $P = 7.84E^{-10}$ ), Stearman Lung ( $n = 20$ ,  $P = 9.97E^{-5}$ ), and Su Lung ( $n = 27$ ,  $P = 1.57E^{-4}$ ), comparing with normal lung tissues (Figure 1C-H). The above data suggested that *ICT1* might play a potential carcinogenesis in LC.

### Immature Colon Carcinoma Transcript 1 Is Widely Expressed in Human LC Cell Lines

To study the function of *ICT1* in human LC, we first examined the expression levels of *ICT1* in 5 LC cell lines 95D, A549,

H1299, H460, and SPC-A-1 by quantitative real-time polymerase chain reaction (qRT-PCR) analysis. As shown in Figure 2A, *ICT1* mRNA was expressed in all 5 cell lines, and the higher transcription levels of *ICT1* were found in NSCLC cell lines 95D and A549 than that in the other 3 cell lines. Therefore, we chose 95D and A549 cells as the target cells for the following *ICT1* biological effect study.

### Knockdown of *ICT1* Expression in NSCLC Cells

To investigate the role of *ICT1* in LC, the expression of *ICT1* was specifically silenced in NSCLC cell line 95D and A549 via lentivirus-mediated RNAi. As shown in Figure 2B, more than 80% cells expressed GFP in NC, *shICT1*(S1), and *shICT1*(S2) groups in both 95D and A549 cells, suggesting a satisfactory infection rate. Knockdown efficiency was further evaluated by qRT-PCR and Western blot analysis. The result (Figure 2C, D) showed that *ICT1* expression on both of mRNA and protein levels was significantly decreased in 2 *shICT1*(S1) and

sh*ICT1*(S2) groups compared with that in the NC group in 95D ( $P < .01$ ) and A549 cells ( $P < .001$ ). The inhibition rate was 98.2% and 88.9% in sh*ICT1*(S1) and sh*ICT1*(S2) groups in 95D cells and was 99.1% and 92.6% in sh*ICT1*(S1) and sh*ICT1*(S2) groups in A549 cells by qRT-PCR, respectively.

### Effect of *ICT1* Knockdown on Cell Growth

To confirm whether *ICT1* was related to 95D and A549 cell proliferation, the effects of *ICT1* knockdown on cell growth were assessed using MTT analysis. As depicted in Figure 3A and B, the growth rate of 95D and A549 cells transduced with sh*ICT1* was significantly inhibited in a time-dependent manner ( $P < .001$ ). The number of sh*ICT1*(S1)- and sh*ICT1*(S2)-infected 95D cells was reduced by 81% and 56%, respectively. And the number of A549 cells was reduced by 50% and 37% in sh*ICT1*(S1) and sh*ICT1*(S2) groups, respectively. Furthermore, the effect of *ICT1* knockdown on colony formation of 95D and A549 cells was determined by crystal violet staining. As shown in Figure 3C, both the size and the number of sh*ICT1*-infected cells exhibited a significant decrease in the colony formation ability of the 95D and A549 cells. Statistical analysis showed the number of colonies in sh*ICT1*(S1) and sh*ICT1*(S2) groups were markedly fewer compared with those in the NC group in both 95D and A549 cells ( $P < .001$ ; Figure 3D).

### Knockdown of *ICT1* Arrested Cell Cycle Progression

To explain the underlying mechanisms of inhibition of cell growth, flow cytometry with PI staining was used to analyze phases of cell cycle of 95D and A549 cells infected with sh*ICT1*(S1). As shown in Figure 4A, the percentage of cells in G<sub>0</sub>/G<sub>1</sub> phase was decreased from 49.04%  $\pm$  0.17% in shCon-infected 95D cells to 29.65%  $\pm$  0.20% in sh*ICT1*(S1) 95D cells, whereas that in G<sub>2</sub>/M phase was increased from 8.53%  $\pm$  0.24% in shCon-infected 95D cells to 31.98%  $\pm$  0.49% in sh*ICT1*(S1)-infected 95D cells. Moreover, compared to the NC group, the cell percentage in sh*ICT1*(S1)-infected A549 cells was increased in G<sub>0</sub>/G<sub>1</sub> phase (67.83%  $\pm$  0.10% vs 61.78%  $\pm$  0.64%) and G<sub>2</sub>/M phase (13.82%  $\pm$  0.31% vs 11.25%  $\pm$  0.60%), whereas decreased in S phase (18.35%  $\pm$  0.31% vs 26.97%  $\pm$  0.60%; Figure 4B). In addition, 0.14%  $\pm$  0.03% cells were detected at sub-G<sub>1</sub> phase in sh*ICT1*(S1)-infected 95D cells, much higher than those in NC-infected cells (0.06%  $\pm$  0.03%). And we also found the cell population in sub-G<sub>1</sub> phase (0.38%  $\pm$  0.18%) was increased in the sh*ICT1*(S1) group in comparison with the NC group (0.11  $\pm$  0.09%) in A549 cells. These results suggested *ICT1* knockdown could inhibit NSCLC cell growth by inducing cell cycle arrest and might induced early cell apoptosis.

### Knockdown of *ICT1* Altered the Expression of G<sub>0</sub>/G<sub>1</sub>-Related Cell Cycle Regulators

To investigate the cause of cell cycle progression arrest, we determined the expression of cell cycle inhibitor p21 and cell

cycle activator cyclin D1 using Western blot analysis. As shown in Figure 3B, the protein expression of p21 was remarkably upregulated in sh*ICT1*(S1)-infected 95D cells compared with that in NC-infected 95D cells. What's more, the protein expression of cyclin D1 was obviously downregulated in sh*ICT1*(S1)-infected 95D cells compared with that in NC-infected 95D cells.

### Knockdown of *ICT1* Induces Cell Apoptosis in NSCLC Cells

To further confirm the effect of *ICT1* silencing on cell apoptosis, we applied annexin V-APC/7-AAD double staining in 95D and A549 cells infected with NC, sh*ICT1*(S1), and sh*ICT1*(S2) groups. As shown in Figure 5A and B, the percentage of early apoptotic cells was increased from 8.10%  $\pm$  0.35% to 15.27%  $\pm$  0.85% in sh*ICT1*(S1) group and from 8.10%  $\pm$  0.35% to 10.70%  $\pm$  0.10% in sh*ICT1*(S2) group in 95D cells in comparison with that in the NC group. Likewise, compared with the NC group, the percentage of late apoptotic cells in 95D cells was increased from 10.13%  $\pm$  1.59% to 28.90%  $\pm$  2.62% in sh*ICT1*(S1) group and from 10.13%  $\pm$  1.59% to 16.70%  $\pm$  0.95% in the sh*ICT1*(S2) group. Similar to the results in 95D cells, the cell percentage of apoptosis was observed a significant increase in the sh*ICT1*(S1) group (early apoptosis: 2.44%  $\pm$  0.33% vs 0.45%  $\pm$  0.12%, late apoptosis: 0.11%  $\pm$  0.07% vs 0.00%  $\pm$  0.01%) and sh*ICT1*(S2) group (early apoptosis: 5.31  $\pm$  0.31% vs 0.45  $\pm$  0.12%, late apoptosis: 1.09  $\pm$  0.24% vs 0.00  $\pm$  0.01%) compared with those in the NC group in A549 cells (Figure 5C and D). The aforementioned results suggested that *ICT1* gene silencing could induce a strong apoptotic effect in human NSCLC cells.

## Discussion

Non-small cell lung cancer is the major type of LC, with less than 15% survival rate for 5 years. Emerging evidence have suggested that some functional molecules have been thought as promising biomarkers for the diagnosis and treatment of patients with NSCLC, which are involved in cell proliferation and cell cycle control.<sup>24</sup> Immature colon carcinoma transcript 1 has been found to be overexpressed in various kinds of cancer cells.<sup>7,25</sup> Network analysis of gene expression by Huang *et al* shows that *ICT1* is a potential biomarker for LC.<sup>10</sup> However, the role of *ICT1* in NSCLC cells remains unclear.

RNA interference has been used as a hopeful therapeutic tool for eliminating cancer-related genes. However, the administration of siRNA often has poor stability, low transfection efficiency, and poor tissue penetration.<sup>26</sup> Therefore, it is important to determine which method is the most efficient and straightforward delivery strategy of the siRNA. Lentiviral-mediated expression systems have been confirmed that it could encode siRNA as a common means of supplying long-term gene silencing.<sup>27</sup> Moreover, lentivirus-mediated RNAi used to silence *ICT1* expression has been regarded as an underlying therapeutic method for human glioblastoma therapy.<sup>9</sup> In this

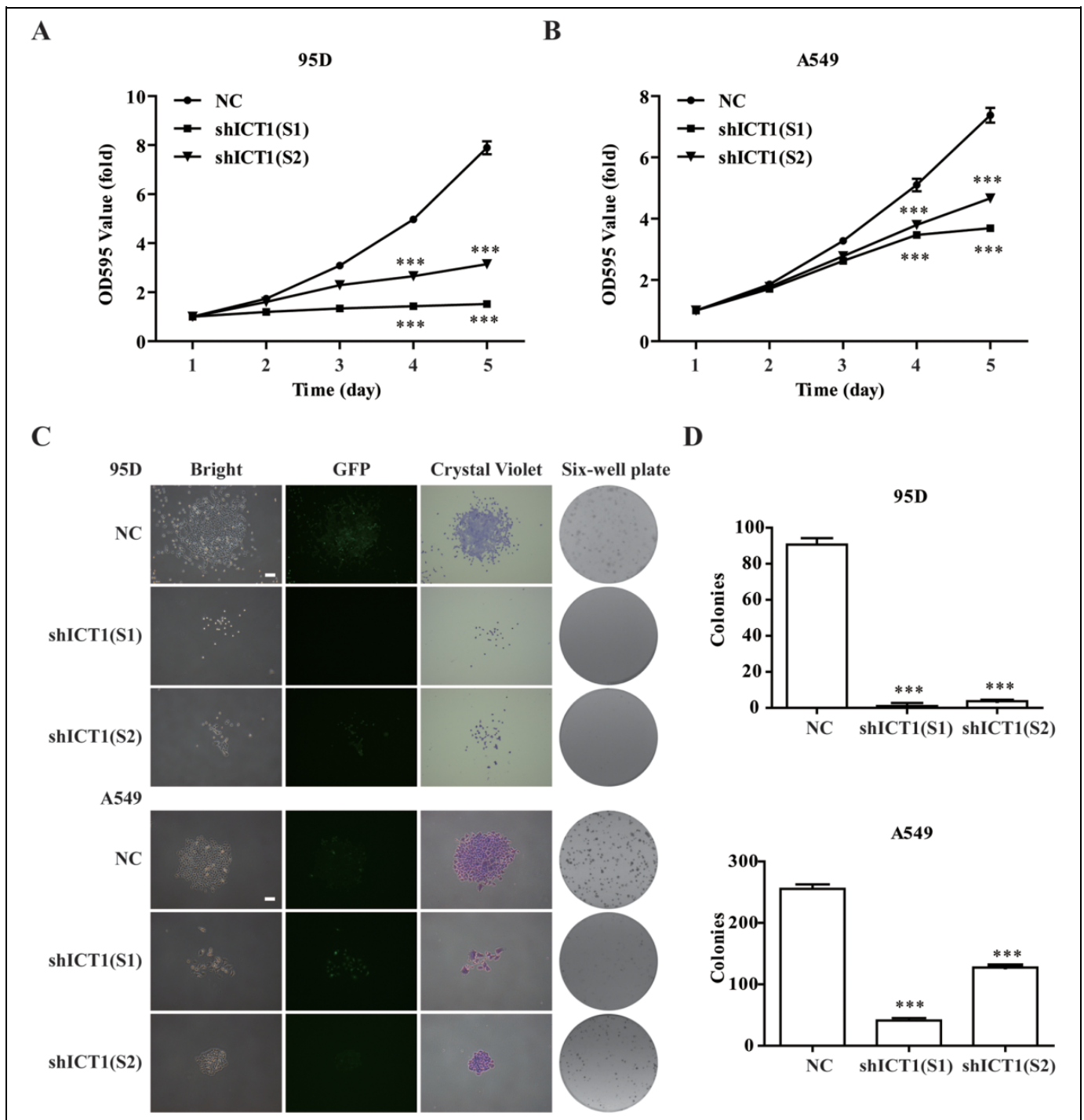


**Figure 3.** Knockdown of immature colon carcinoma transcript 1 (*ICT1*) knockdown inhibited cell growth. A and B, The *ICT1* knockdown significantly inhibited 95D and A549 cell proliferation confirmed by MTT. After infection for 96 hours, 95D and A549 cells transfected with negative control (NC) or sh*ICT1* group were reseeded into 96-well plates. MTT was added followed by 4 hours of incubation once daily for 5 days. The optical density (OD) value at 595 nm was measured. C and D, The *ICT1* knockdown significantly suppressed colony formation ability in 95D and A549 cells confirmed by colony formation assay. After infection for 96 hours, 95D and A549 cells were reseeded into 6-well plates at 400 cells per well to form colonies. The corresponding colony numbers in different groups (NC, sh*ICT1*[S1], and sh*ICT1*[S2]) were counted and recorded. The colonies stained with crystal violet were captured under a light microscopy. \*\*\* $P < .001$ ; scale bar, 25  $\mu$ m.

study, *ICT1* was identified as a specific molecule that could drive NSCLC progression using lentivirus-mediated RNAi technology. Knockdown of *ICT1* significantly suppressed cell

viability and colony formation ability of 95D and A549 cells, which suggested *ICT1* was an indispensable factor for cell proliferation in NSCLC. As our best knowledge, human

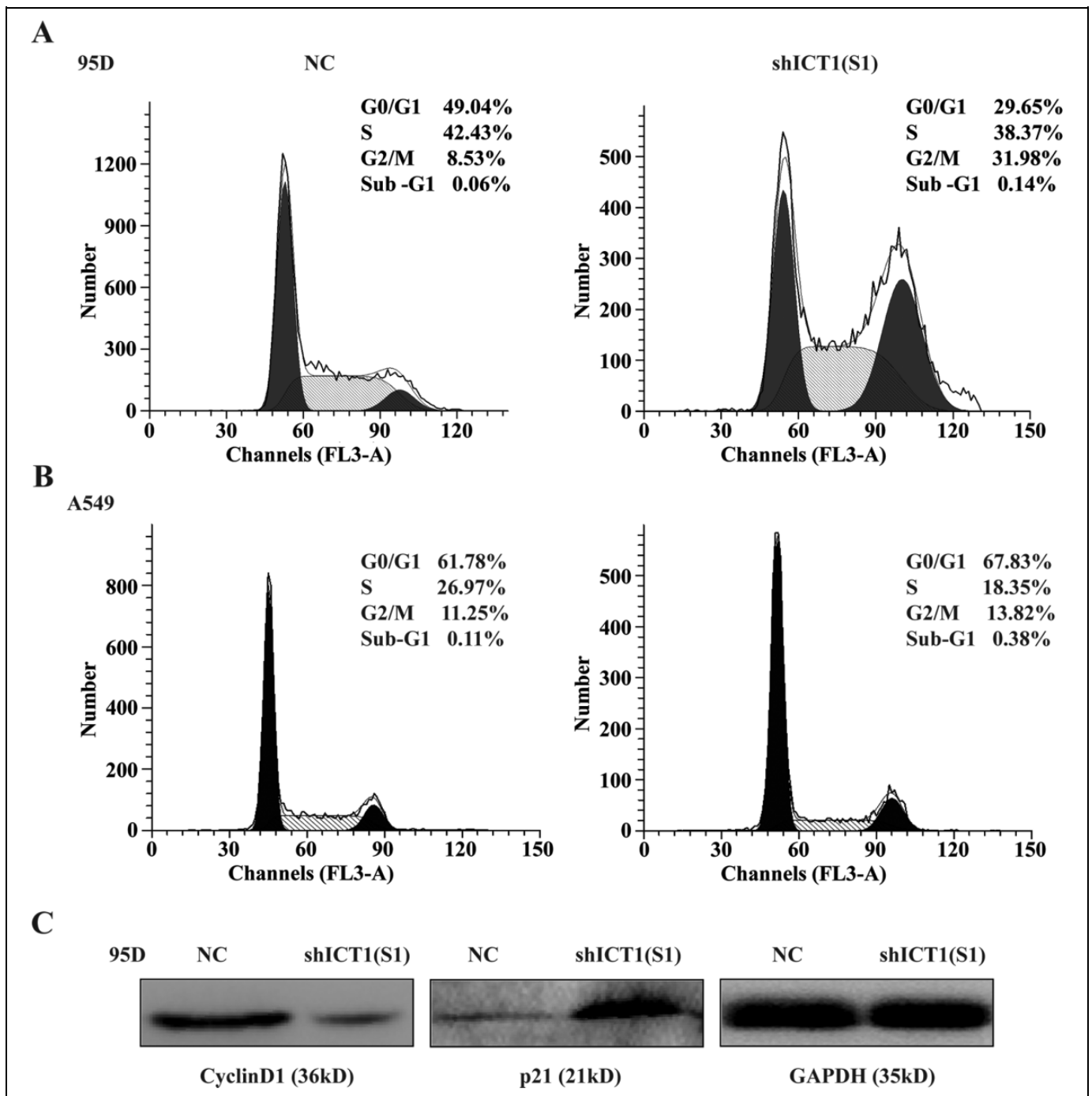


**Figure 4.** Knockdown of immature colon carcinoma transcript 1 (*ICT1*) arrested cell cycle progression. A and B, The percentage of 95D and A549 cells in each phase of the cell cycle. The 95D and A549 cells were infected with negative control (NC) or sh*ICT1*(S1) group for 5 days, and the cell cycle distribution was measured using propidium iodide (PI) staining and flow cytometry analysis. C, The expression of downstream proteins, including cyclin D1 and p21, were assayed by Western blot after infection with NC or sh*ICT1*(S1) for 5 days.

mitochondria are ubiquitous organelles essential for cell viability and its dysfunction results in cell proliferation inhibition and apoptosis.<sup>28</sup> Immature colon carcinoma transcript 1 is an essential mitochondrial protein and its knockdown may result in a decrease in mitochondrial protein synthesis leading to suppress cell viability.<sup>6,7</sup> In accordance with our study, cell

proliferation and colony formation ability were remarkably inhibited in prostate cancer and GBM cells after *ICT1* knockdown.<sup>8,9</sup>

To further uncover the causes of *ICT1* on cell proliferation, the percentage of cells in cell cycle distribution was analyzed in 95D and A549 cells after *ICT1* knockdown using flow



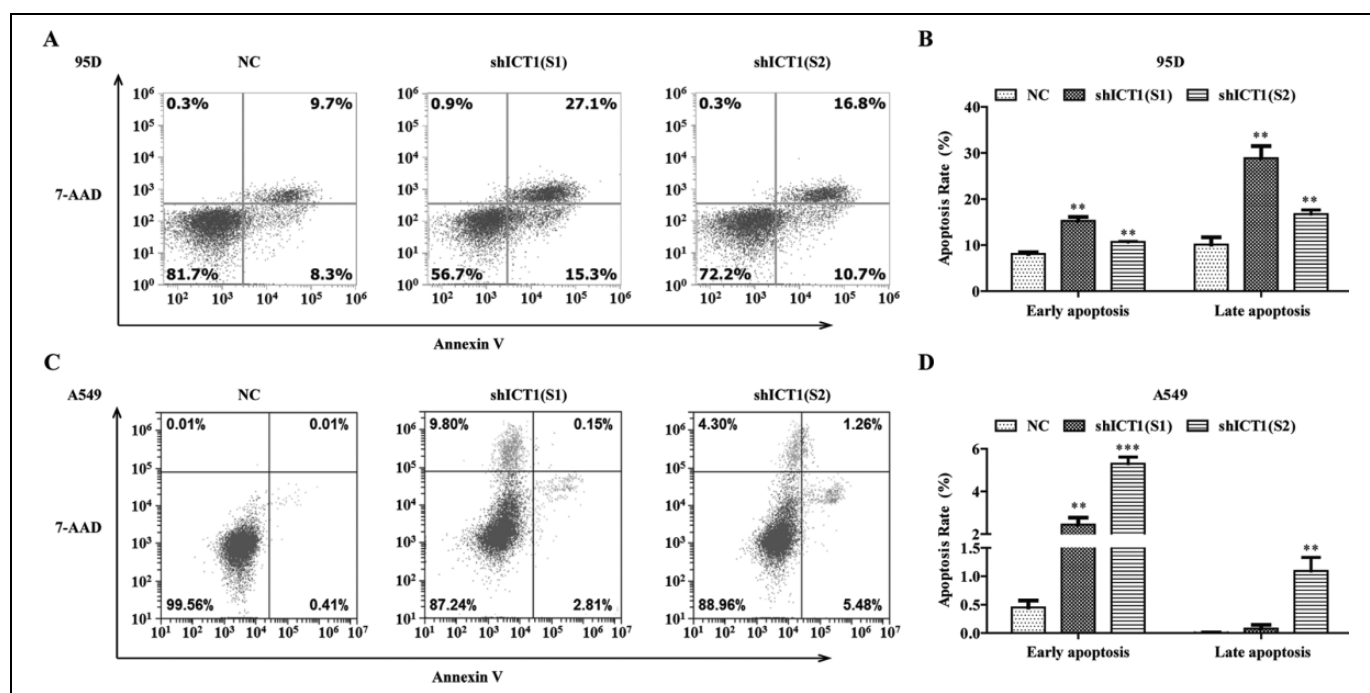


**Figure 5.** Knockdown of immature colon carcinoma transcript 1 (ICT1) promoted cell apoptosis in non-small cell lung cancer (NSCLC) cells. A and B, Flow cytometry was used to evaluate apoptotic cells. The 95D and A549 cells were infected with NC, shICT1(S1), and shICT1(S2) groups for 5 days, and the cell apoptosis was measured using annexin V-APC/7-AAD double staining. C and D, Statistical analysis of early and late apoptotic cells in NSCLC cells. \*\* $P < .01$ ; \*\*\* $P < .001$ .

cytometry. Our results showed *ICT1* silencing arrested cell cycle at G2/M phase in 95D cells while at G<sub>0</sub>/G<sub>1</sub> phase in A549 cells. The difference may be due to the different cell derivation that 95D cells belong to high spontaneous metastasis of LC cells,<sup>29</sup> whereas A549 cells is from a 58-year-old Caucasian male, which could synthesize lecithin with a high content of unsaturated fatty acid.<sup>30</sup> In addition, we found knockdown of *ICT1* suppressed the expression of cyclin D1 and increased the expression of p21. Cyclin D1, as a member of the cyclin D, plays a key role in promoting cell cycle and presents upregulation in a variety of tumor tissues.<sup>31,32</sup> Cyclin D1 also regulates the G<sub>1</sub>/S phase transition of the cell cycle and is essential for the initiation of mitosis.<sup>33</sup> In our study, the expression of cyclin D1 was decreased in *ICT1* knockdown cells, which suggested that *ICT1* knockdown-arrested cell cycle may be partly through the suppression of cyclin D1. As G1 phase regulator, p21 has been demonstrated to be a cell cycle inhibitor.<sup>34</sup> Combined with the above analysis, we could infer p21 presented upregulation along with downregulation of cyclin D1 in blocking cell cycle. Furthermore, we found more cells accumulated in sub-G<sub>1</sub> phase, which is usually considered to be the result of apoptotic DNA fragmentation. We may conclude that knockdown of *ICT1* induced mitochondrial-related apoptosis leading to cell growth inhibition and early apoptosis. In accordance with the result of sub-G<sub>1</sub> phase, annexin V/7-AAD double staining analysis indicated that *ICT1* silencing could promote NSCLC cell apoptosis. These data are supported by the report of Handa *et al.*<sup>7</sup> Further research is needed to explore the further molecular mechanism of *ICT1*

in LC. In addition, other limitations that are presented in this study such as absence of *ICT1* overexpression and without *in vivo* animal experiments remain to be determined in further research.

In summary, our preliminary study reveals the important role of *ICT1* in NSCLC cells that knockdown of *ICT1* significantly suppressed cell proliferation, arrested cell cycle through altering expression cell cycle regulators, and promoted cell apoptosis. Immature colon carcinoma transcript 1 may be a critical molecule in the occurrence of NSCLC, and it will be valuable to further investigate the potential application of *ICT1* targeted therapy in more preclinical and clinical NSCLC studies.

#### Authors' Note

Yiling Wang and Jiantao He have contributed equally to this study.

#### Declaration of Conflicting Interests

The author(s) declared no potential conflicts of interest with respect to the research, authorship, and/or publication of this article.

#### Funding

The author(s) received no financial support for the research, authorship, and/or publication of this article.

#### References

- Siegel R, Naishadham D, Jemal A. Cancer statistics, 2013. *CA Cancer J Clin.* 2013;63(1):11-30.

2. Zhan C, Yan L, Wang L, et al. Identification of immunohistochemical markers for distinguishing lung adenocarcinoma from squamous cell carcinoma. *J Thorac Dis.* 2015;7(8):1398-1405. doi:10.3978/j.issn.2072-1439.2015.07.25.
3. Xu JH, Yang HP, Zhou XD, et al. Autophagy accompanied with bisdemethoxycurcumin-induced apoptosis in non-small cell lung cancer cells. *Biomed Environ Sci.* 2015;28(2):105-115. doi:10.3967/bes2015.013.
4. Ge L, Shi R. Progress of EGFR-TKI and ALK/ROS1 inhibitors in advanced non-small cell lung cancer. *Int J Clin Exp Med.* 2015; 8(7):10330-10339.
5. Sakuma T, Barry MA, Ikeda Y. Lentiviral vectors: basic to translational. *Biochem J.* 2012;443(3):603-618. doi:10.1042/BJ20120146.
6. Richter R, Rorbach J, Pajak A, et al. A functional peptidyl-tRNA hydrolase, ICT1, has been recruited into the human mitochondrial ribosome. *EMBO J.* 2010;29(6):1116-1125. doi:10.1038/emboj.2010.14.
7. Handa Y, Hikawa Y, Tochio N, et al. Solution structure of the catalytic domain of the mitochondrial protein ICT1 that is essential for cell vitality. *J Mol Biol.* 2010;404(2):260-273. doi:10.1016/j.jmb.2010.09.033.
8. Wang Z, Xu D, Gao Y, et al. Immature colon carcinoma transcript 1 is essential for prostate cancer cell viability and proliferation. *Cancer Biother Radiopharm.* 2015;30(7):278-284. doi:10.1089/cbr.2014.1728.
9. Xie R, Zhang Y, Shen C, et al. Knockdown of immature colon carcinoma transcript-1 inhibits proliferation of glioblastoma multiforme cells through Gap 2/mitotic phase arrest. *Onco Targets Ther.* 2015;8:1119-1127. doi:10.2147/OTT.S75864.
10. Huang P, Cao K, Zhao H. Screening of critical genes in lung adenocarcinoma via network analysis of gene expression profile. *Pathol Oncol Res.* 2014;20(4):853-858. doi:10.1007/s12253-014-9764-z.
11. Rhodes DR, Yu J, Shanker K, et al. ONCOMINE: a cancer microarray database and integrated data-mining platform. *Neoplasia.* 2004;6(1):1-6.
12. Bhattacharjee A, Richards WG, Staunton J, et al. Classification of human lung carcinomas by mRNA expression profiling reveals distinct adenocarcinoma subclasses. *Proc Natl Acad Sci U.S.A.* 2001;98(24):13790-13795. doi:10.1073/pnas.191502998.
13. Landi MT, Dracheva T, Rotunno M, et al. Gene expression signature of cigarette smoking and its role in lung adenocarcinoma development and survival. *PLoS One.* 2008;3(2): e1651. doi:10.1371/journal.pone.0001651.
14. Beer DG, Kardia SL, Huang CC, et al. Gene-expression profiles predict survival of patients with lung adenocarcinoma. *Nat Med.* 2002;8(8):816-824. doi:10.1038/nm733.
15. Stearman RS, Dwyer-Nield L, Zerbe L, et al. Analysis of orthologous gene expression between human pulmonary adenocarcinoma and a carcinogen-induced murine model. *Am J Pathol.* 2005;167(6):1763-1775. doi:10.1016/S0002-9440(10)61257-6.
16. Su LJ, Chang CW, Wu YC, et al. Selection of DDX5 as a novel internal control for Q-RT-PCR from microarray data using a block bootstrap re-sampling scheme. *BMC Genomics.* 2007;8: 140. doi:10.1186/1471-2164-8-140.
17. Hou J, Aerts J, den Hamer B, et al. Gene expression-based classification of non-small cell lung carcinomas and survival prediction. *PLoS One.* 2010;5(4): e10312. doi:10.1371/journal.pone.0010312.
18. Selamat SA, Chung BS, Girard L, et al. Genome-scale analysis of DNA methylation in lung adenocarcinoma and integration with mRNA expression. *Genome Res.* 2012;22(7):1197-1211. doi:10.1101/gr.132662.111.
19. Okayama H, Kohno T, Ishii Y, et al. Identification of genes upregulated in ALK-positive and EGFR/KRAS/ALK-negative lung adenocarcinomas. *Cancer Res.* 2012;72(1): 100-111. doi:10.1158/0008-5472.CAN-11-1403.
20. Rhodes DR, Kalyana-Sundaram S, Mahavisno V, et al. OncoPrint 3.0: genes, pathways, and networks in a collection of 18,000 cancer gene expression profiles. *Neoplasia.* 2007;9(2):166-180.
21. Arocho A, Chen B, Ladanyi M, Pan Q. Validation of the 2- $\Delta\Delta C_t$  calculation as an alternate method of data analysis for quantitative PCR of BCR-ABL P210 transcripts. *Diagn Mol Pathol.* 2006; 15(1):56-61.
22. Xu J, Yang Y, Hao P, Ding X. Claudin 8 contributes to malignant proliferation in human osteosarcoma U2OS cells. *Cancer Biother Radiopharm.* 2015;30(9):400-404. doi:10.1089/cbr.2015.1815.
23. Xu M, Wang Y, Chen L, et al. Down-regulation of ribosomal protein S15A mRNA with a short hairpin RNA inhibits human hepatic cancer cell growth in vitro. *Gene.* 2014;536(1):84-89.
24. Wang LE, Yin M, Dong Q, et al. DNA repair capacity in peripheral lymphocytes predicts survival of patients with non-small-cell lung cancer treated with first-line platinum-based chemotherapy. *J Clin Oncol.* 2011;29(31):4121-4128. doi:10.1200/JCO.2010.34.3616.
25. Chen R, Wang Y, Liu Y, et al. Quantitative study of the interactome of PKC $\zeta$  involved in the EGF-induced tumor cell chemotaxis. *J Proteome Res.* 2013;12(3):1478-1486. doi:10.1021/pr3011292.
26. Ran R, Liu Y, Gao H, et al. PEGylated hyaluronic acid-modified liposomal delivery system with anti-gamma-glutamylcyclotransferase siRNA for drug-resistant MCF-7 breast cancer therapy. *J Pharm Sci.* 2015;104(2):476-484. doi:10.1002/jps.24163.
27. Abbas-Terki T, Blanco-Bose W, Deglon N, et al. Lentiviral-mediated RNA interference. *Hum Gene Ther.* 2002;13(18): 2197-2201. doi:10.1089/104303402320987888.
28. Mandal S, Guptan P, Owusu-Ansah E, Banerjee U. Mitochondrial regulation of cell cycle progression during development as revealed by the tenured mutation in *Drosophila*. *Dev Cell.* 2005; 9(6):843-854. doi:10.1016/j.devcel.2005.11.006.
29. Lu YL. Spontaneous metastasis of clonal cell subpopulations of human lung giant cell carcinoma after subcutaneous inoculation in nude mice [in Chinese]. *Zhonghua Zhong Liu Za Zhi.* 1989; 11(1):1-7.
30. Giard DJ, Aaronson SA, Todaro GJ, et al. In vitro cultivation of human tumors: establishment of cell lines derived from a series of solid tumors. *J Natl Cancer Inst.* 1973;51(5):1417-1423.

31. Loden M, Stighall M, Nielsen NH, et al. The cyclin D1 high and cyclin E high subgroups of breast cancer: separate pathways in tumorigenesis based on pattern of genetic aberrations and inactivation of the pRb node. *Oncogene*. 2002;21(30):4680-4690.
32. Caldon CE, Musgrove EA. Distinct and redundant functions of cyclin E1 and cyclin E2 in development and cancer. *Cell Div*. 2010;5:2. doi:10.1186/1747-1028-5-2.
33. Zhao S, Yi M, Yuan Y, et al. Expression of AKAP95, Cx43, CyclinE1 and CyclinD1 in esophageal cancer and their association with the clinical and pathological parameters. *Int J Clin Exp Med*. 2015;8(5):7324-7332.
34. Abe R, Beckett J, Abe R, et al. Olive oil polyphenol oleuropein inhibits smooth muscle cell proliferation. *Eur J Vasc Endovasc Surg*. 2011;41(6):814-820. doi:10.1016/j.ejvs.2010.12.021.